AgriEngineering

MDPI

Article

Optimizing Orchard Planting Efficiency with a GIS-Integrated Autonomous Soil-Drilling Robot

Osman Eceoğlu [1] and İlker Ünal [2,*]

[1] Department of Control and Automation, Technical Science Vocational School, Akdeniz University, 07070 Antalya, Turkey; osmaneceoglu@akdeniz.edu.tr
[2] Department of Mechatronics, Technical Science Vocational School, Akdeniz University, 07070 Antalya, Turkey
* Correspondence: ilkerunal@akdeniz.edu.tr; Tel.: +905-069-289-903

Abstract: A typical orchard's mechanical operation consists of three or four stages: lining and digging for plantation, moving the seedling from nurseries to the farm, moving the seedling to the planting hole, and planting the seedling in the hole. However, the digging of the planting hole is the most time-consuming operation. In fruit orchards, the use of robots is increasingly becoming more prevalent to increase operational efficiency. They offer practical and effective services to both industry and people, whether they are assigned to plant trees, reduce the use of chemical fertilizers, or carry heavy loads to relieve staff. Robots can operate for extended periods of time and can be highly adept at repetitive tasks like planting many trees. The present study aims to identify the locations for planting trees in orchards using geographic information systems (GISs), to develop an autonomous drilling machine and use the developed robot to open planting holes. There is no comparable study on autonomous hole planting in the literature in this regard. The agricultural mobile robot is a four=wheeled nonholonomic robot with differential steering and forwarding capability to stable target positions. The designed mobile robot can be used in fully autonomous, partially autonomous, or fully manual modes. The drilling system, which is a y-axis shifter driven by a DC motor with a reducer includes an auger with a 2.1 HP gasoline engine. SOLIDWORKS 2020 software was used for designing and drawing the mobile robot and drilling system. The Microsoft Visual Basic.NET programming language was used to create the robot navigation system and drilling mechanism software. The cross-track error (XTE), which determines the distances between the actual and desired holes positions, was utilized to analyze the steering accuracy of the mobile robot to the drilling spots. Consequently, the average of the arithmetic means was determined to be 4.35 cm, and the standard deviation was 1.73 cm. This figure indicates that the suggested system is effective for drilling plant holes in orchards.

Keywords: agricultural robotics; GIS; orchard; precision agriculture; soil-drilling machine

check for updates

Citation: Eceoğlu, O.; Ünal, İ. Optimizing Orchard Planting Efficiency with a GIS-Integrated Autonomous Soil-Drilling Robot. *AgriEngineering* **2024**, *6*, 2870–2890. https://doi.org/10.3390/agriengineering6030166

Academic Editor: Simone Pascuzzi

Received: 24 June 2024
Revised: 7 August 2024
Accepted: 9 August 2024
Published: 13 August 2024

Copyright: © 2024 by the authors. Licensee MDPI, Basel, Switzerland. This article is an open access article distributed under the terms and conditions of the Creative Commons Attribution (CC BY) license (https://creativecommons.org/licenses/by/4.0/).

1. Introduction

The aim of agricultural mechanization is to reduce dependence on labor, increase farm productivity, speed up field operations, and achieve high income while minimizing costs [1]. Automation and precise management technologies have significantly improved agriculture during the last few decades. The implementation of automation and precision management, however, has not been focused on specialized crops, such as tree fruit, because orchard tasks are difficult and orchard systems are inconsistent [2]. For this reason, human labor continues to be a major component of most tree fruit-producing operations. Meanwhile, more food must be produced to feed a population that is growing steadily while there are fewer resources available, such as water and agricultural areas. Whatever happens in the orcharding sector, in order to reduce the production inputs and environmental impact of agricultural systems, precision agriculture has become crucial in today's dynamic environment. Precision agriculture has been applied extensively to field crops and is

becoming increasingly popular among academics and industry participants working with tree fruit crops [3]. As a result, intelligent mechanical and automated systems are the answers to the problems facing the tree fruit sector, as they lower the need for labor.

Agricultural production areas, whether plant production areas or orchards, have a complex and heterogeneous structure. The development of agricultural robotic systems depends heavily on the environment in which the robots will be used, as system complexity increases in cost. In the last few years, numerous research institutes have created robot tractors and mobile robots for different agricultural purposes. Even though orchard platforms have been demonstrated to increase productivity, their limited applicability and high cost in relation to the advantages they offer have prevented them from being widely adopted. A shared mobile platform that can be utilized in fully manual, partially manual, or totally autonomous modes is crucial for the orchard environment. This kind of technology is feasible and will increase efficiency in a variety of applications [4]. Orchards appear to be the best location for implementing robots and automated systems in agriculture due to their organized environment [5]. Furthermore, a serious danger to orchard industries is the declining availability of skilled labor for seasonal orchard tasks. For this reason, it is critical to develop robotic orchard solutions [6]. Many studies on the automation of various orchard tasks, such as spraying and harvesting, have been conducted over the past fifty years. The majority of these research studies focus on a single task [7]. There are numerous automated harvesting robot prototypes for orchards [8–12]. Additionally, there are also studies in the literature on robotic tasks like thinning [13], spraying [14], pruning [15], and mobile navigation [16] in orchard environments. Every orchard management operation listed above requires a mobile platform in order to move the actuators around the orchard. Mobile platforms must be precisely navigated through orchards. In addition to accurately guiding robots from point A to point B within the orchard, the system must consider simultaneous manipulations directed towards the trees or fruits. Precise orchard maps are essential for accurate mobile robot localization in orchards because they enable the robot to navigate between tree rows by accurately estimating its position and orientation [17]. The mapping of the orchard can also be utilized to create an autonomous navigation system that uses an appropriate control strategy to manage the mobility of the mobile robot within the orchard. As a result, an a priori environment map is required for all the navigation and localization techniques for mobile robot platforms.

Mobile robots must be able to successfully navigate through feature extraction, mapping, localization, path planning, and obstacle avoidance in orchard environments. Using its onboard sensors, a mobile robot can map the orchard and identify its surroundings, updating the map in real time. Accurate orchard maps are crucial for agricultural robots' navigation, localization, and path planning. The accuracy of the orchard map can be increased by integrating several sensors for developing the feature extraction and mapping of the orchard. The process of precisely calculating a mobile robot's attitude in relation to an environment map using information gathered from the robot's sensors is known as localization [18]. Reliability in gathering sensor data and their automatic association with the environment map constitute the basis of the localization challenge. All the navigation and localization expressions explained above indicate that an environmental map should be created starting from the establishment phase of the orchards. Global Navigation Satellite Systems (GNSSs)-based technologies and GISs are becoming increasingly popular among farmers these days for their farming tasks, particularly in the area of landscape design. Software known as a GIS (geographic information system) 10.5 is designed specifically to work with spatial data and enable the creation of intricate, scaled maps with quantifiable features [19]. The core of an orchard planting plan, which is about comprehending and creatively planning the natural and artificial topography of a particular place, is closely tied to a GIS [20]. In this respect, a GIS can be regarded as an instrument to create orchard planting maps and in the development of orchard planning research and design.

An orchard layout is a plan that illustrates how the plants are arranged in an orchard. Any orchard design strategy should accommodate the greatest number of plants and pro-

vide enough space for the orchard's easy cultural operations [21]. Planting systems can be broadly classified into two categories: the vertical system of planting and the alternate-row planting system. The first tree in the vertical system of planting is precisely perpendicular to the trees in the orchard's subsequent rows. The vertical systems of planting include square and rectangular systems. The alternate row planting system is used when the trees in the neighboring row are not quite vertical. This planting method includes the quincunx, triangular, and hexagonal systems. The most effective and economical management of the orchard requires a meticulous plan. The optimum spacing to accommodate the maximum number of trees per unit area can be the result of good planning [22]. The simplest and most widely used planting method for fruit trees is the square system. Trees are planted in this technique on every corner of a square, regardless of the planting distance (the space between plants and rows remains the same). The similarity in distances between trees and rows (5 × 5 m, 6 × 6 m, etc.) allows for the execution of intercultural operations in both directions. Establishing an orchard begins with selecting the suitable planting method and correctly marking the planting spots [23]. Geospatial analysis, which includes methods and techniques for analyzing data in their spatial context, is regarded as the fundamental component of a GIS [24]. A GIS can assist farmers in effectively managing their orchard design strategy, in providing the planting coordinates of trees for autonomous tree planting, and in creating coordinate maps for autonomous subsequent orchard operations.

It is challenging to complete the afforestation sector's massive work volume solely through manual labor due to the requirement to afforest ever-larger areas in orchards [25]. Especially, digging holes for tree planting is a laborious and time-consuming task. In the future, planting more trees will be required over even larger areas. Modern horticulture applications use a wide range of automation techniques to make operations simple and staff-free. Nevertheless, no research has been conducted on an autonomous robot that digs holes for the planting of seedlings in the context of orchard establishment. The current soil-drilling machines on the market are not always able to drill perpendicular to the ground and are difficult to operate. The mobility of a soil-drilling machine is limited, which makes using it by one person much more challenging. In addition, it has become a necessity to design them autonomously due to reasons such as low performance on rough surfaces, difficulties in transportation, and security problems due to open designs. However, there is no mobile robot system available in the market or the literature that can autonomously drill planting holes using maps. Based on the planting map generated by the GIS software, the developed mobile robot navigates to the drilling spots on its own and drills holes. This study's conceptual structure is presented in Figure 1.

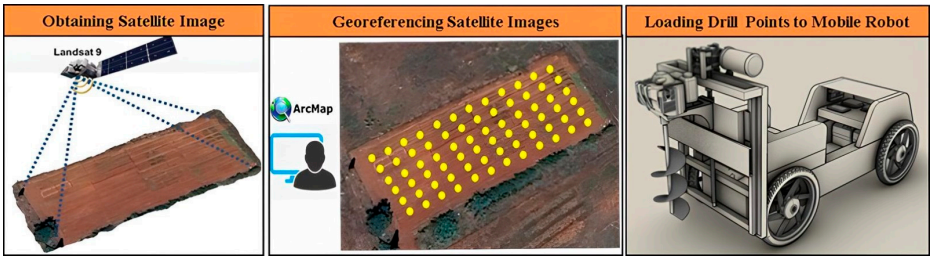


Figure 1. This study's conceptual structure for marking drilling points from satellite images and drilling with a mobile robot.

2. Materials and Methods

The digital image data of the study field taken from the Landsat satellite was used to enable the developed GIS-based soil-drilling robot to function autonomously in the orchard. The coordinates of the spots where the robot would drill holes were identified using the ArcMap application on the digital satellite image, and a task file was generated. The generated task file was loaded to the onboard computer of the mobile robot. A navigation program was developed so that the mobile robot can move autonomously in the study field. The mobile robot was autonomously steered to the holes location, and it drilled the holes

using the navigation program according to the coordinates in the task file. The photograph of the GIS-based autonomous soil-drilling robot is shown in Figure 2. The primary objective of this paper is to employ ArcGIS 10.5 software to determine the geographic locations of the sapling holes in the orchard and to ensure the development and adaptation of the autonomous mobile robot and soil auger machine. There are four primary structures in the system:

1. Development of the autonomous mobile robot and navigation algorithm: The four-wheeled autonomous robot is steered by four DC motors. It has a differential steering mechanism. It can be maneuvered manually or autonomously from point to point.
2. Adaptation of the autonomous mobile robot and soil auger machine: The soil auger machine is a specially designed solution for the task of drilling soil; it is a modification of the autonomous mobile robot that we previously developed.
3. Determination of drilling spots of planting holes on the digital map: Drilling spots of planting holes were determined using ArcGIS 10.5 software to handle and merge data, carry out detailed analysis, and model and automate procedural operations.
4. The designed system's software solutions: The software is designed to enable autonomous navigation of the mobile robot and operation of the auger system.

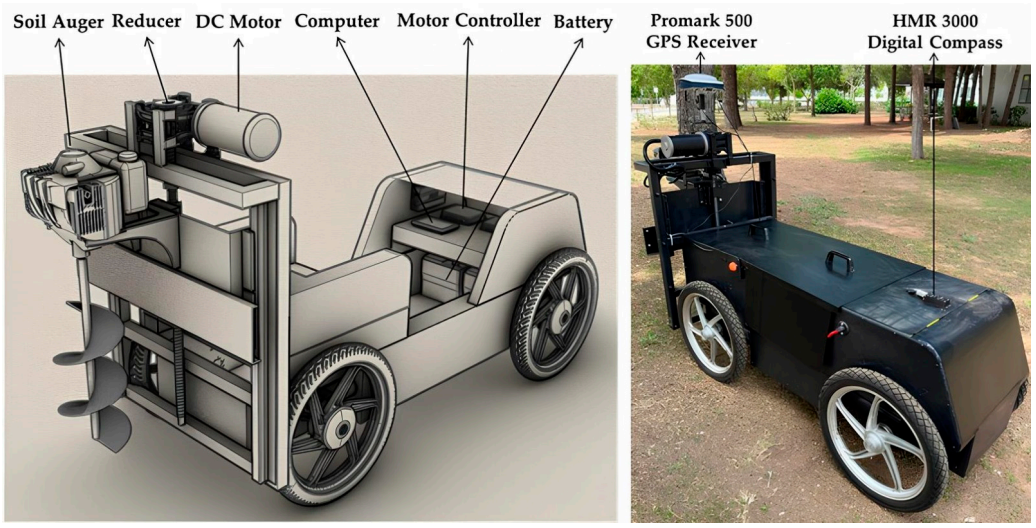


Figure 2. Equipment used on GIS-based autonomous soil-drilling robot and photo of the developed robot.

2.1. Autonomous Mobile Robot and Navigation Algorithm

The agricultural mobile robot, which has four wheels, can be maneuvered both manually and automatically. To steer the robot under field circumstances, four rubber wheels measuring 2.50 × 17 were selected. During field operations, the traction and overall driving performance of the machine are significantly impacted by the wheel characteristics of the machine. It is a well-known fact that reducing the detrimental impact of heavy agricultural machinery on soil compaction requires large wheel widths. But, especially in orchards, narrow wheels should be used for inter-row operations. Wider wheels may result in pressure being put on seedlings during driving, and the increased wheel width will lead to an increase in the torque of the vehicle. The increasingly widespread use of agricultural mobile robots has brought many challenges with completing agricultural tasks. Among them is the fact that they have an effective amount of an energy source, especially a battery, to maintain motion and mission planning, for long-term or difficult tasks will not be completed as intended if there is insufficient energy. The mobile robot's efficient use of its available energy became crucial due to the rising demand for energy. The total weight of the robot is approximately 150 kg, which balances stability and mobility, essential for accurate and efficient operation in the field. For the movement of wide wheels, more torque is required. Increased torque shortens the mobile robot's operating time by forcing

the DC motors to draw more power from the battery. Because of this, wide wheels were not used in order to extend the life of the mobile robot battery.

The steering mechanism of the mobile robot is differential. The right front motor of the mobile robot is connected to the right rear motor, and the left front motor is connected to the left rear motor in an electrical series configuration. In this arrangement, the right and left motors are operated differentially, enabling the mobile robot to utilize a differential driving system. The robot's left and right wheels can move at different speeds from one another. All of the wheels' speeds need to match for the mobile robot to steer in a straight line. The robot turns to the side of the slowest wheel if the left and right wheels are moving at different speeds. The mobile robot can turn 360 degrees in its current location by rotating its left and right wheels in opposition to one another. Four 24 V, 0.25 kW, 1440 rpm DC motors are used to power the mobile robot. The mobile robot's electric motor output for traction is 1 kW in total. This power distribution between the four wheels allows the mobile robot to deliver traction power without excessively draining the battery. They are connected to a 1:10 reduction gearbox. The mobile robot is equipped with motor–gearbox assemblies installed on its chassis, to which each wheel is connected independently. This allows the wheels to receive all of the torque produced by the motors. The torque of the gear reducer is 16.58 Nm. The shaft torque is 34.99 Nm. The robot has a maximum speed of 15.2 km/h and weighs about 150 kg when batteries and the measurement system are included. To guide the mobile robot, two RoboteQ FDC3260 3-channel DC motor control units (Roboteq Inc., Scottsdale, AZ, USA) are utilized to adjust the motors' speed and direction. The RoboteQ FDC3260 is an advanced motor controller for high-performance electric vehicle applications. It is capable of handling up to 60 V and 60 A per channel, which allows it to manage significant power levels, essential for demanding drive applications. The FDC3260 features numerous inputs and outputs, including analog, digital, and pulse, along with RS232, USB, and CAN bus interfaces, which facilitate robust and versatile communication options. Furthermore, the FDC3260 integrates advanced safety mechanisms such as emergency stop, voltage, temperature monitoring, and fault detection features, which help ensure safe operation under a variety of conditions. The mobile robot and other equipment are powered by two 12 V-72 Ah sealed, rechargeable, maintenance-free batteries (Mutlu Battery Inc., Istanbul, Turkey). The batteries are standard car batteries. In addition, two batteries are linked in series to give the DC motors 24 V. A technical drawing of the mobile robot is presented in Figure 3.

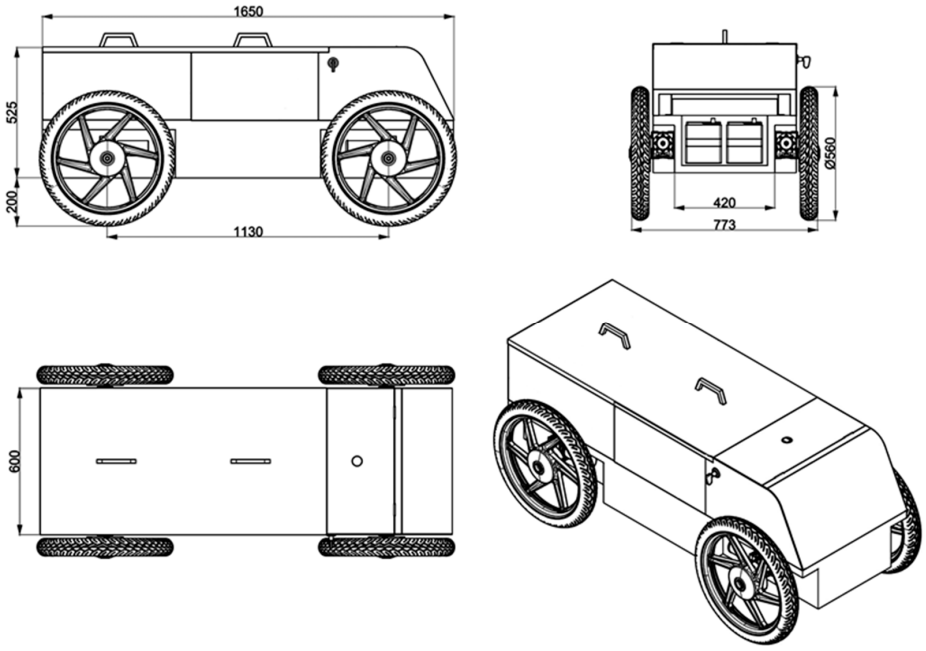


Figure 3. Top, front, and side views of the technical drawing of the mobile robot.

The mobile robot's energy consumption and operating time calculation are given Table 1. This calculation assumes that the robot operates continuously under orchard conditions, cycling between the 250 W motors and the 500 W motor, with all other components running constantly. The mobile robot's operating time is approximately 3.53 h. During this period, the mobile robot can open approximately 270 seedling holes.

Table 1. Mobile robot energy consumption and operating time calculation.

Component	Current Draw (A)	Duration (s)	Total Current Seconds (A·s)
250 W motors	3	7	21
500 W motor	15	40	600
Other components	7.185	47	337.695
Total			958.695

The calculation steps for the energy consumption of the mobile robot are given below:

1. Calculate total current draw per component: First, determine how much current each component draws during its operation. This involves multiplying the current draw by the duration each component is active in a given cycle.
2. Total current seconds ($A{\cdot}s$) calculation for each component:
   - 250 W motors: These motors draw 3 A and operate for 7 s. Current seconds = $3\,A \times 7\,s = 21\,A{\cdot}s$.
   - 500 W motor: This motor draws 15 A and operates for 40 s. Current seconds = $15\,A \times 40\,s = 600\,A{\cdot}s$.
   - Other components (including the industrial computer, motor control card, and compass): These draw a total of 7.185 A and run continuously. For a cycle of 47 s: current seconds = $7.185\,A \times 47\,s = 337.695\,A{\cdot}s$.
3. Calculate total current seconds for the cycle: total current seconds = 21 + 600 + 337.695 = $958.695\,A{\cdot}s$.
4. Total current seconds to amper-hours (Ah):

$$\text{Total Ah per Cycle} = \frac{958.695}{3600} = 0.266\ \text{Ah}$$

5. Operating time: Given the battery capacity and the total amper-hours per cycle, calculating how long the system can operate before the battery is depleted.

$$t = \frac{\text{Total Battery Capacity}}{\text{Ah per Cycle}} = \frac{72\ Ah}{0.0266\ Ah} \times 47\ s = 12701.88\ s$$

6. Working time in hours:

$$\text{t} = \frac{12701.88}{3600} = 3.53\ \text{h}$$

Geographical data for the autonomous steering system were gathered using a Promark 500 RTK-GPS receiver (Magellan Co., Santa Clara, CA, USA). Up to 20 Hz data output rate and 75 channels were available on the receiver. The ProMark 500 GPS receiver is a high-precision device commonly used in geospatial applications such as surveying, mapping, and construction. The ProMark 500 features RTK (Real-Time Kinematic) capability, providing centimeter-level accuracy in real-time data collection. Additionally, the receiver is designed with robustness in mind, featuring a rugged housing suitable for fieldwork in various weather conditions. The ProMark 500 also includes long battery life, which is critical for extended field operations, ensuring that users can work uninterrupted throughout the day. The mobile robot is steered to drilling locations using geographic data (latitude, longitude, speed, time, etc.) obtained from the GPS receiver. The digital compass Honey-

well HMR3200 (Honeywell International Inc., Charlotte, NC, USA) was utilized to obtain the robot's precise heading angle for navigation software. The RTK-GPS system and digital compass ensure high-precision navigation, requiring robust but lightweight components to maintain maneuverability. The Honeywell HMR3200 integrates sensors for detecting magnetic fields along three axes and accelerometers for tilt compensation, enabling it to provide accurate heading information regardless of its orientation. The device operates over a wide range of temperatures, making it suitable for various environmental conditions. With its low power consumption, the HMR3200 is ideal for battery-operated applications such as handheld navigation devices, marine electronics, and robotics. Additionally, it features a serial communication interface for easy integration with other systems and devices. The most crucial element for minimizing mobile robot turns is quadrant control. There are four different ranges of degrees on the compass dial: quadrant 1 is 0 to 90 degrees, quadrant 2 is 90 to 180 degrees, quadrant 3 is 180 to 270 degrees, and quadrant 4 is 270 to 360 (or 0) degrees. Based on quarter control, the mobile robot determines whether to move straight forward, left, or right. This control is made according to which quadrant the robot and the target point are in [26]. The quadrant control mechanism's flowchart is shown in Figure 4.

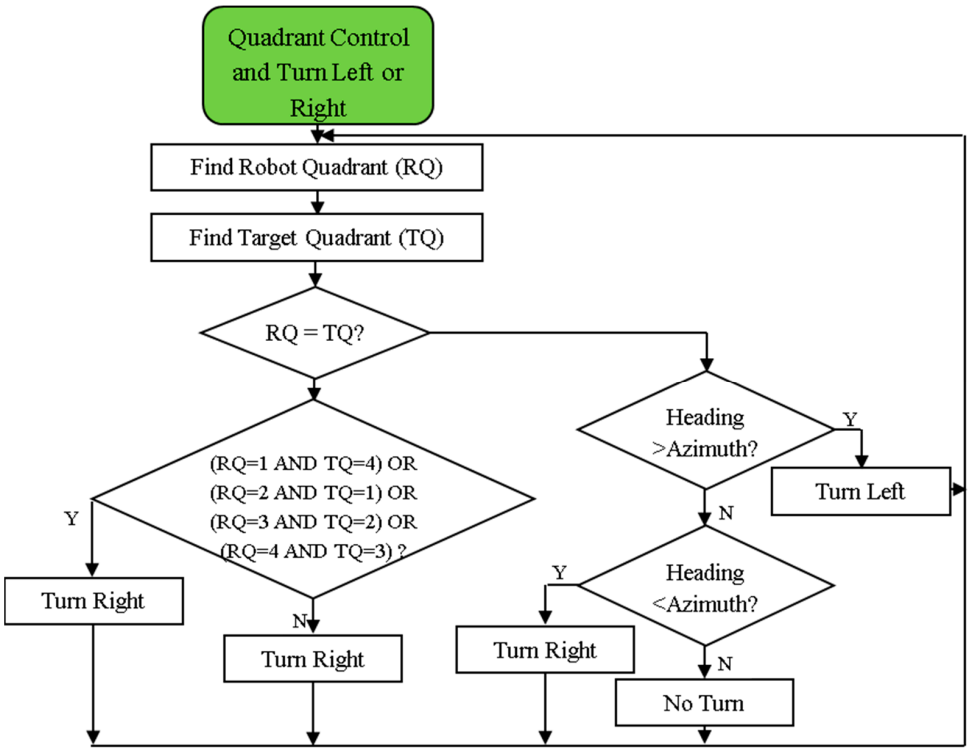


Figure 4. The quadrant control mechanism's flowchart [26].

The heading angle is the angle in the horizontal plane formed between the present direction of a mobile robot's longitudinal axis and north, whether it is magnetic or true north. The angle between north and the destination point is known as the azimuth. The heading and azimuth angles are used to determine the angle difference. The azimuth and heading angle difference is computed instantaneously by the navigation algorithm. The mobile robot can be guided in the desired direction in this manner. The distance between the target point and the mobile robot location is then computed. Finally, the mobile robot reaches its destination when the heading angle equals the azimuth angle and the distance equals zero. The flowchart for the mobile robot navigation method is shown in Figure 5.

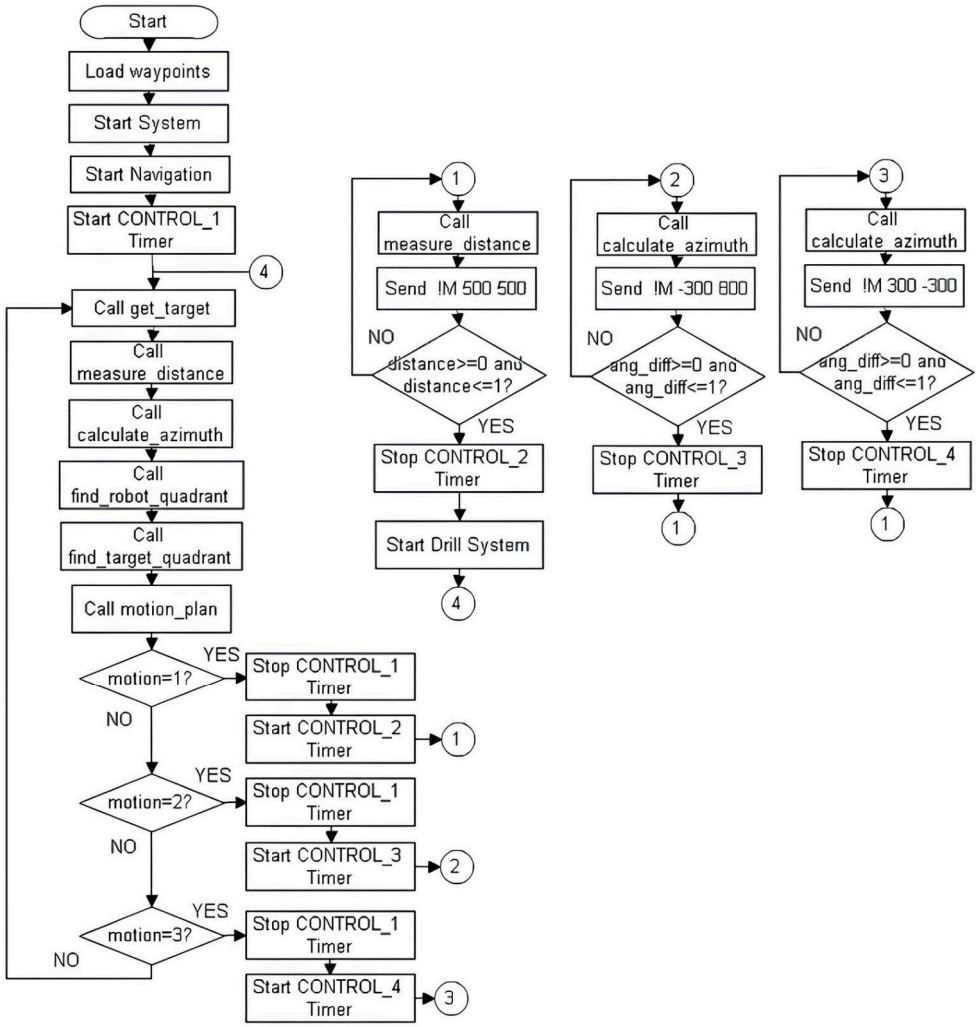


Figure 5. The flowchart for the mobile robot navigation method.

2.2. Adaptation of the Autonomous Mobile Robot and Soil Auger Machine

An instrument for drilling holes in the earth is called a soil auger. Usually, it is made out of a vertical metal rod or pipe that rotates and has one or more blades attached to the lower end of it to scrape or cut the soil. A GIS-based autonomous mobile robot that may be used to drill holes for planting trees, installing telephone or electricity poles, and other suitable tasks, is the idea behind this work. We decided that it is more acceptable to combine our built autonomous mobile robot with the gasoline-powered hole drilling equipment that is currently on the market for this reason. The GIS-based autonomous soil-drilling robot is designed to operate effectively on various soil types, including sandy, clayey, and loamy soils. It can handle soil moisture content ranging from 10% to 60% and soil densities between 1.0 g/cm^3 and 1.9 g/cm^3. These ranges ensure the robot's versatility and efficiency in different agricultural environments. The technical drawings for the mobile robot attached to the soil auger machine are presented in Figure 6.

In this study, the Palmera ZLAG520B soil auger machine (Remaş Inc., Istanbul, Turkey) was coupled to the vertical movement mechanism designed for the rear of the developed mobile robot. The soil auger has the following technical specifications: It features an engine power of 2.1 hp (1.6 kW) and a cylinder volume of 51.7 cm^3 for the soil-drilling mechanism to ensure sufficient power for efficient drilling in various soil types. The auger has a diameter of 20 cm and a depth of 90 cm. It comes with a standard transmission and a fuel tank capacity of 0.8 L. The weight of the machine is 14.8 kg, and it has a reduction ratio of 34:1. Stainless steel was used to construct the vertical movement mechanism. Some

of the mechanisms' parts were made of square steel tube that measured 30 × 30 × 3 mm. The H-shaped carrier grid and the soil auger machine are the two components that make up the system's mechanical structure. Two 30 × 30 910 mm and three 30 × 30 800 mm square steel tubes were used to build an H-shaped carrier grid for the system's vertical movement. Then this H-shaped carrier grid was attached to the rear of the autonomous mobile robot. The soil auger machine was mounted on an H-shaped grid (Figure 7). The two steel linear guides on the H-shaped grid are adjusted by pillow blocks and 30 mm linear rail shaft guide supports. The linear guides have a length of 910 mm. For vertical movement, a 1:40 reduction gearbox was connected to a 24 V, 500 W, 1440 rpm DC motor that drove a 30 × 850 mm ball screw, forming a linear actuator.

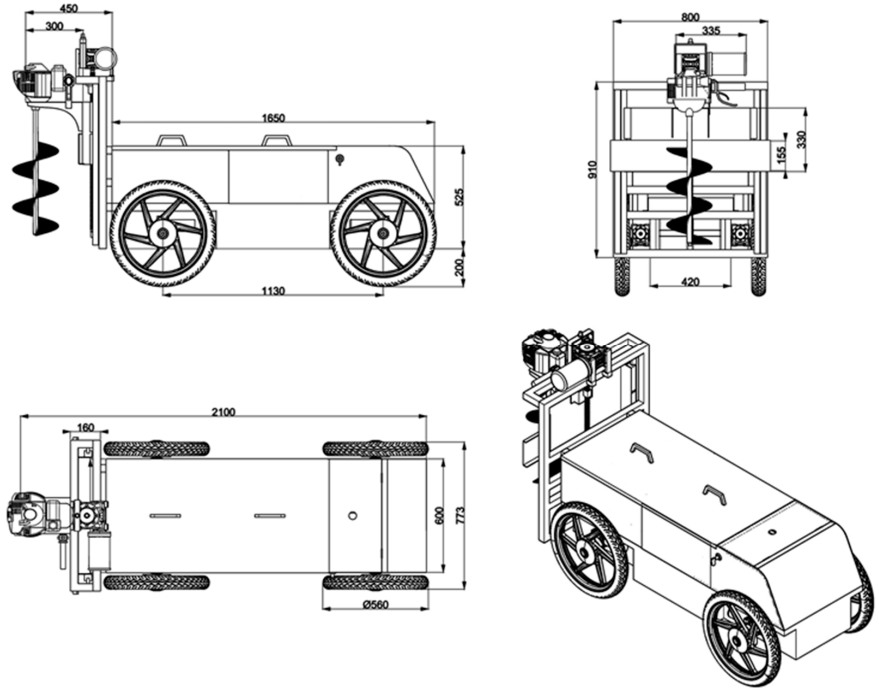


Figure 6. Top, front, and side views of the technical drawings for the mobile robot attached to the soil auger machine.

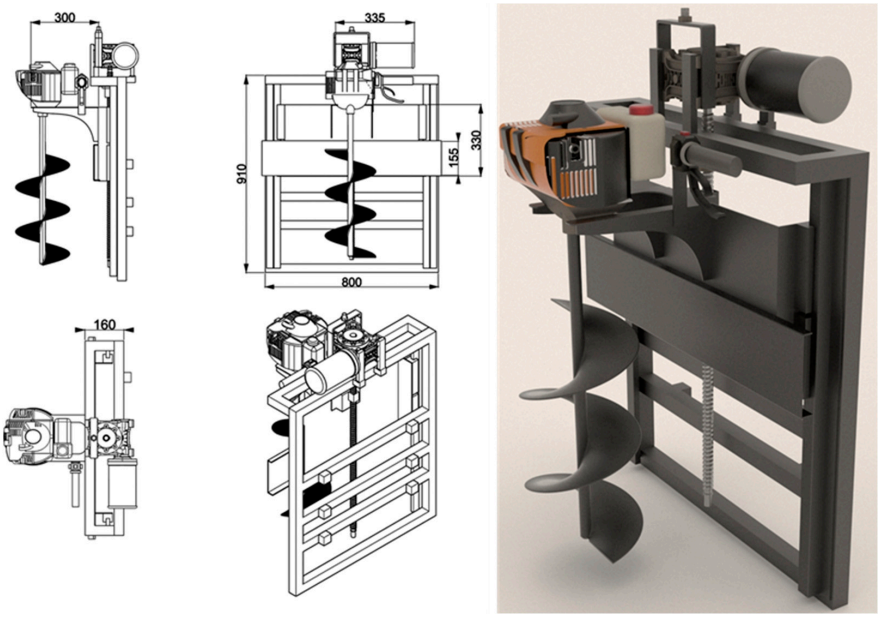


Figure 7. Full-scale technical drawing of the soil auger machine and H-shaped grid.

The developed four-wheel differential driving mobile robot on a two-dimensional plane is displayed in Figure 8. It shows the local coordinate system (X_1, O, Y_1), where Y_1 is the robot's lateral direction, O is the robot's center point, and X_1 is the driving direction.

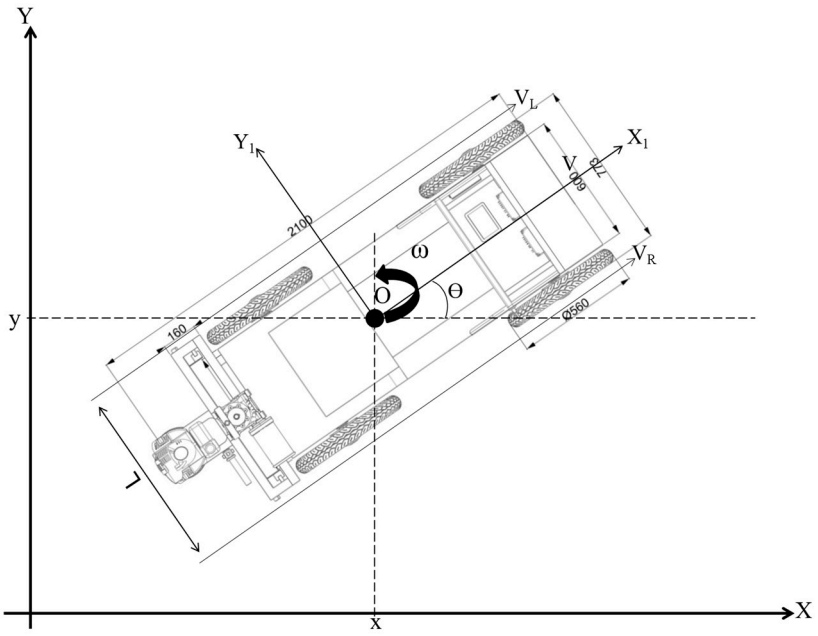


Figure 8. The kinematics schematic of the differential drive mobile robot.

For a nonholonomic 4WD mobile robot, the differential equations of motion can be written as

$$\begin{bmatrix} \dot{x} \\ \dot{y} \\ \dot{\theta} \end{bmatrix} = \begin{bmatrix} \mathrm{Cos}\theta & 0 \\ \mathrm{Sin}\theta & 0 \\ 0 & 1 \end{bmatrix} * \begin{bmatrix} v \\ \omega \end{bmatrix} \quad (1)$$

$$P = \begin{bmatrix} v \\ \omega \end{bmatrix} = \begin{bmatrix} \frac{r}{2} & \frac{r}{2} \\ \frac{r}{L} & -\frac{r}{L} \end{bmatrix} * \begin{bmatrix} v_R \\ v_L \end{bmatrix} \quad (2)$$

Here, the position, velocity, and angular velocity of the mobile robot are represented by ((x, y, θ), v, ω), and their derivatives are denoted by ($\dot{x}$, $\dot{y}$, $\dot{\theta}$), respectively. L denotes the breadth of the left and right wheels, while v_L and v_R, respectively, represent the left and right driving wheels' velocities. Based on the given formula, when $v_R = v_L$ and ω = 0, the robot travels straight at a consistent speed. If $v_R = -v_L$, it will spin around its center of mass. When $v_R \neq v_L$, the robot follows a curved path with a specific radius (ρ). The formula for calculating the radius of this curve is detailed in Equation (3):

$$\rho = \frac{v}{\omega} = \frac{L * (v_L + v_R)}{2 * (v_L - v_R)} \quad (3)$$

Upon reviewing the above equations, the kinematic equation for the nonholonomic mobile robot can be formulated as shown in Equation (4):

$$P = \begin{bmatrix} \dot{x} \\ \dot{y} \\ \dot{\theta} \end{bmatrix} = \begin{bmatrix} \frac{r}{2} * Cos\theta & \frac{r}{2} * Cos\theta \\ \frac{r}{2} * Sin\theta & \frac{r}{2} * Sin\theta \\ \frac{r}{L} & \frac{-r}{L} \end{bmatrix} * \begin{bmatrix} v_R \\ v_L \end{bmatrix} \quad (4)$$

2.3. Determination of Drilling Spots of Planting Holes on the Digital Map

With the aid of a GIS, users can produce interactive maps with multiple layers that are useful for both geographical analysis and the visualization of complicated data. A GIS is essentially the fusion of database technology and mapping. GISs are utilized in urban

planning, emergency management, photogrammetry, cartography, remote sensing, land surveying, and geography. The most important advantages of a GIS for fruit cultivation are the provision of a planned land-use strategy obtained by predetermining the most suitable areas based on products and the preparation of the seedling planting plan. Assessing the aforementioned benefits, it is clear that the first step in implementing autonomous systems for orchards will be planning the planting of trees on a digital map and mapping out the location of seedling holes. In this context, a digital image of the orchard was first imported into the ArcMap program in order to locate the seedling holes. Next, hole locations were marked on the image, separated by 6 m in both the horizontal and vertical orientations (Figure 9). Finally, a database table was created after the coordinate information of the seedling holes was extracted from the image. In order to autonomously guide the mobile robot to the drilling holes, the database table was used as a task file.

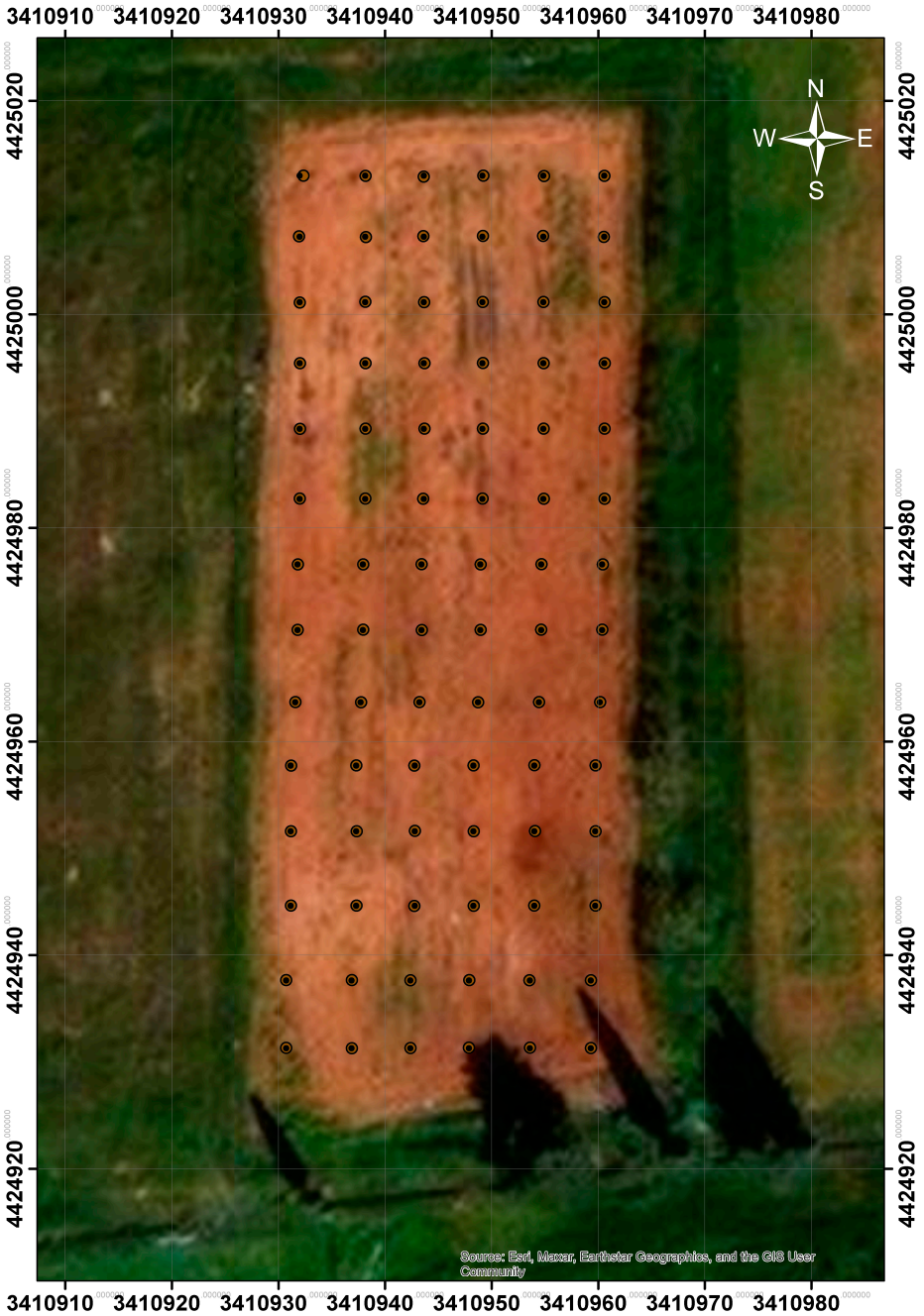
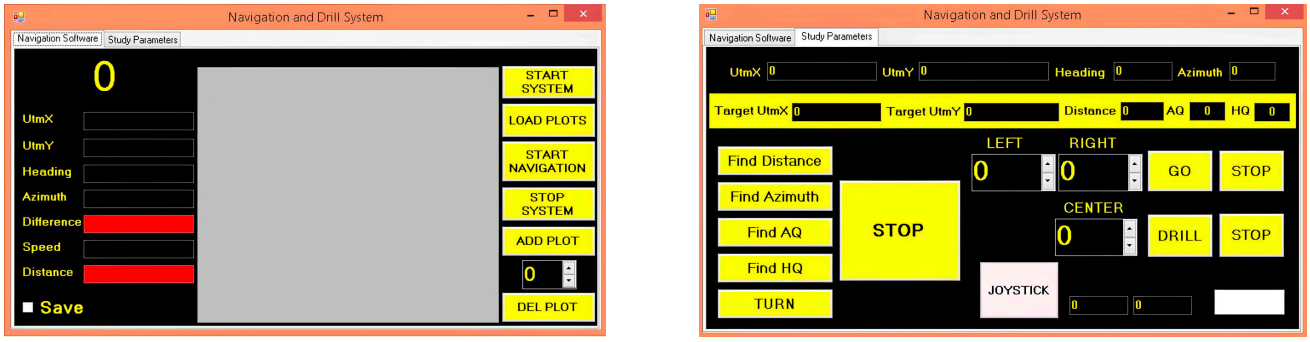


Figure 9. ArcMap program in order to locate the seedling holes.

2.4. The Designed System's Software Solutions

The navigation program was built in Visual Studio.NET 2015 using the Visual Basic.NET language to control the mobile robot both manually and automatically (Figure 10). Furthermore, the developed software instantly activates the soil-drilling mechanism when the mobile robot arrives at the target spot. The occurrence of all of these activities depends on the task file being uploaded to the mobile robot's industrial computer. A task file is a list of points defined by a geographical position, latitude, and longitude coordinates used by the mobile robot navigation. Furthermore, the locations of the drill spots for the soil are indicated by these coordinates as well.



(**a**) (**b**)

Figure 10. Developed navigation and drilling software: (**a**) the software that was designed for mobile robot navigation; (**b**) soil-drilling procedures.

The azimuth angle of the destination point and the robot's heading angle are the two key angles for mobile robot navigation. The navigation program uses the HMR3200 digital compass to determine the heading angle of the robot. It additionally computes the azimuth angle continually. It also computes the distance between the robot position (X_1, Y_1) and the target position (X_2, Y_2). For the purpose of statistically analyzing the discrepancy between the desired drilling spots and the real drilling spots where the robot stops, all location data are stored in the SQL Server 2005 database.

2.5. Field Study Experiment

All experimental evaluations with the developed robot system were performed on land of the University of Akdeniz (36° 53′ 54″ N and 30° 38′ 27″ E). The experimental field is 32 m above sea level and has an area of 3.1 da. The mobile robot was autonomously navigated to 84 distinct spots throughout the investigation in the experimental field. The soil auger was used to dig a planting hole that was 30 cm deep at each spot. The autonomous stop-and-go navigation approach was employed to drill planting holes in this study. The main idea behind the stop-and-go technique is to halt the robot while it is drilling the planting holes. With this approach, the agricultural robot travels to the first drilling spot, stops, digs a hole, and then moves on to the next.

2.6. Data Analysis, Interpretation, and Visualization

The main purpose of the navigation software in mobile robot navigation is to minimize XTE, which allows the robot to precisely approach the destination spot. XTE is utilized to estimate the overall 2D positional error statistics or to make comparisons [27]. XTE is the Euclidean distance between the desired target position and the real position of the robot:

$$\mathrm{XTE} = \sqrt{(X_R - X_{TP})^2 + (Y_R - Y_{TP})^2} \quad (5)$$

The mobile robot's latitude and longitude are represented by the values X_R and Y_R in the equation. The desired target's latitude and longitude are represented by the values X_{TP}

and Y_{TP}. The XTE values' standard deviations and standard errors were calculated for each drilling process. The XTE data acquired for 84 places were interpreted in order to assess the system's overall success. ArcGIS 10.5 software was used for the purpose of visualization.

3. Results

There are two stages to the experimental study of the GIS-based autonomous soil-drilling robot. The first stage involves setting up the task file for the mobile robot by utilizing the ArcMap application in an office setting to find the holes locations that need to be dug in order to plant seedlings. In the second phase, the prepared task file is uploaded to the mobile robot computer, after which it autonomously goes to the drilling locations one after the other and drills the holes. In the study area, a total of 84 seedling drilling locations with ranges of 6 × 6 m were identified for the task file. The target locations and the locations where the mobile robot drills a hole are displayed in Figure 11. No data were lost because of a weak GPS signal. The operating duration of the mobile robot is roughly 3.53 h. In this time frame, it is capable of creating about 270 seedling holes. The calculations presented here consider maximum speeds. In the field study, engine speeds were halved. Under these conditions, it was observed that the mobile robot operated continuously for approximately 5 h without interruption.

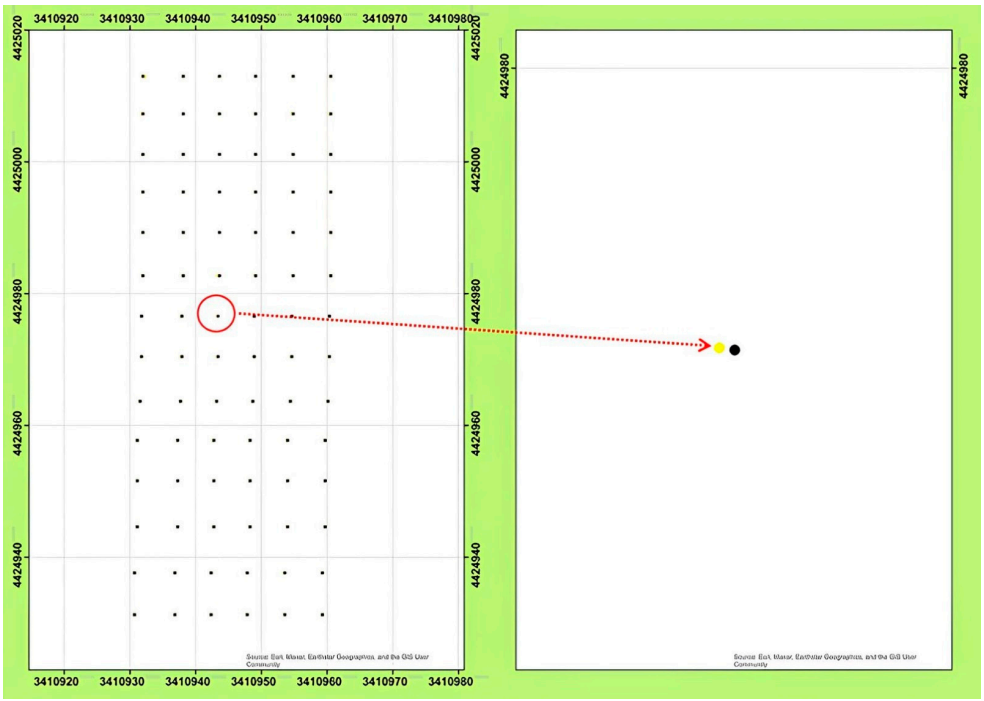


Figure 11. The target locations and the locations where the mobile robot drills a hole.

The mobile robot's images in the study field for the hole drilling-hole operation are displayed in Figure 12. The drilled holes are approximately 20 cm in width and 30 cm in depth. However, attaching augers with varying diameters to the drilling mechanism allows for the opening of deeper and wider holes. The images of the drilled holes are shown in Figure 13.

Data visualization is often achieved through the use of histograms. Histograms are graphical depictions of data collection that indicate the frequency at which each value appears. The histogram of XTE values between the location where the mobile robot digs a hole and the intended digging point is displayed in Figure 14. For a total of 84 spots, the minimum and maximum XTE values were calculated to be 2.41 and 9.41 cm, respectively. The data's standard deviation was computed to be 1.73 cm. Also, the data's mean was computed to be 4.35 cm. It is seen that the majority of XTE values are found to be stuck

between 2.51 cm and 5.96 cm. It is important to know the shape of our datasets on the histogram. Positive or right-skewed graphs have a tail that seems to be pulled to the right. Positively skewed data are characterized by a large number of values that are near the lower end of the range and a rare occurrence of higher values. This indicates that the data mean is usually higher than the median and that the distribution is not symmetrical. When Figure 14 is examined, it is observed that the histogram is positive or right-skewed. For this dataset, the skewness is 1.38 and the kurtosis is 4.07, which indicates moderate skewness and kurtosis. It can see that the largest frequencies of XTE were in the 2.51–5.96 cm range, with a longer tail to the right than to the left. The characteristic of the data reflected in this histogram is significant to understand at which points the position errors of the mobile robot increase.



Figure 12. The mobile robot's images in the study field for hole-drilling operation.



Figure 13. The images of the drilled holes.

One kind of graphic that we can use to determine whether or not a set of data may have originated from a theoretical distribution is the quantile–quantile (Q-Q) plot. A dataset's univariate normality can be determined by looking at the points on the normal QQ plot. A 45-degree reference line will be where the points fall if the data are normally distributed. In the event that the data are not normally distributed, the points will deviate from the line of reference. The corresponding quantile values of the dataset are represented on the y axis of the normal QQ plot in Figure 15 below, while the quantile values of the standard normal distribution are plotted on the x axis. It can be seen that the points almost fall close to the 45-degree reference line. The main departure from this line occurs at high values of XTE. Right-skewed data show up as a concave curve on a normal Q-Q plot. The x axis represents the theoretical quantiles of the standard normal distribution. This axis has values ranging

from −2.51 to +2.51, which are the expected minimum and maximum quantile values for a standard normal distribution. The y axis represents the quantiles of the observed dataset. In this study, the data values vary approximately from 2.51 to 9.41 cm. As observed in the graph, most points are close to the line, indicating that the dataset largely conforms to a normal distribution. However, there are deviations, especially at the extremes. Such deviations suggest the presence of outliers or non-normal behavior at the tails of the dataset, indicating possible extreme values or different behaviors at the dataset's ends.

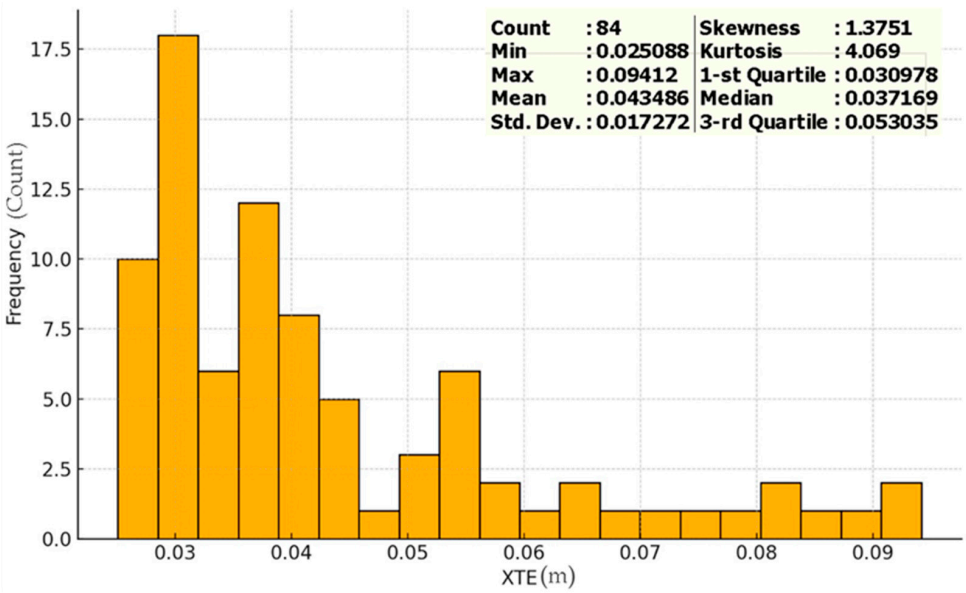


Figure 14. Histogram of the XTE values of the mobile robot. The x axis of the histogram represents the range of XTE values of the mobile robot. The y axis represents the frequency or count of XTE values.

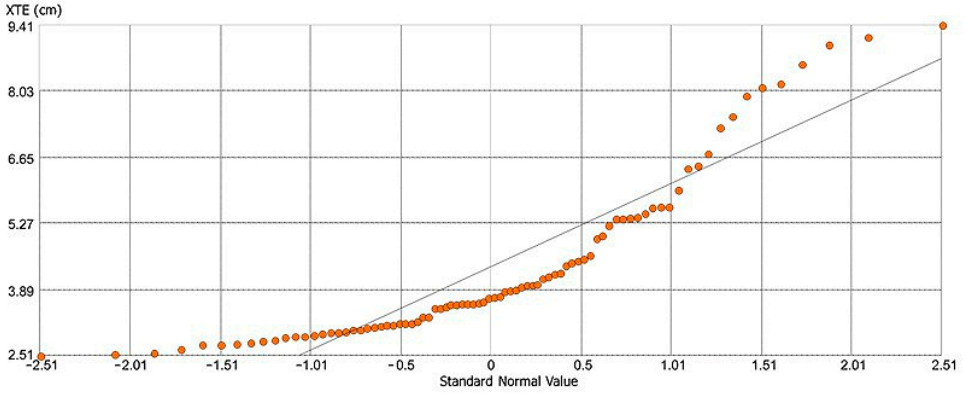


Figure 15. Normal QQ plot of XTE values. This Q–Q plot compares the XTE values on the vertical axis to a statistical population on the horizontal axis.

The simple kriging method was used to understand the differences to the research area. Simple kriging is less complex than ordinary kriging, yet it produces a smoother result by averaging of the entire dataset. No general trends were subtracted, nor were the data values transformed or declustered to produce regularity. The spatial distribution of the XTE is shown in Figure 16. It shows that the XTE is less than 4.7 cm in a significant part of the studied area. This indicates that the GIS-based autonomous soil-drilling robot may function in the work area with reasonable XTE errors.

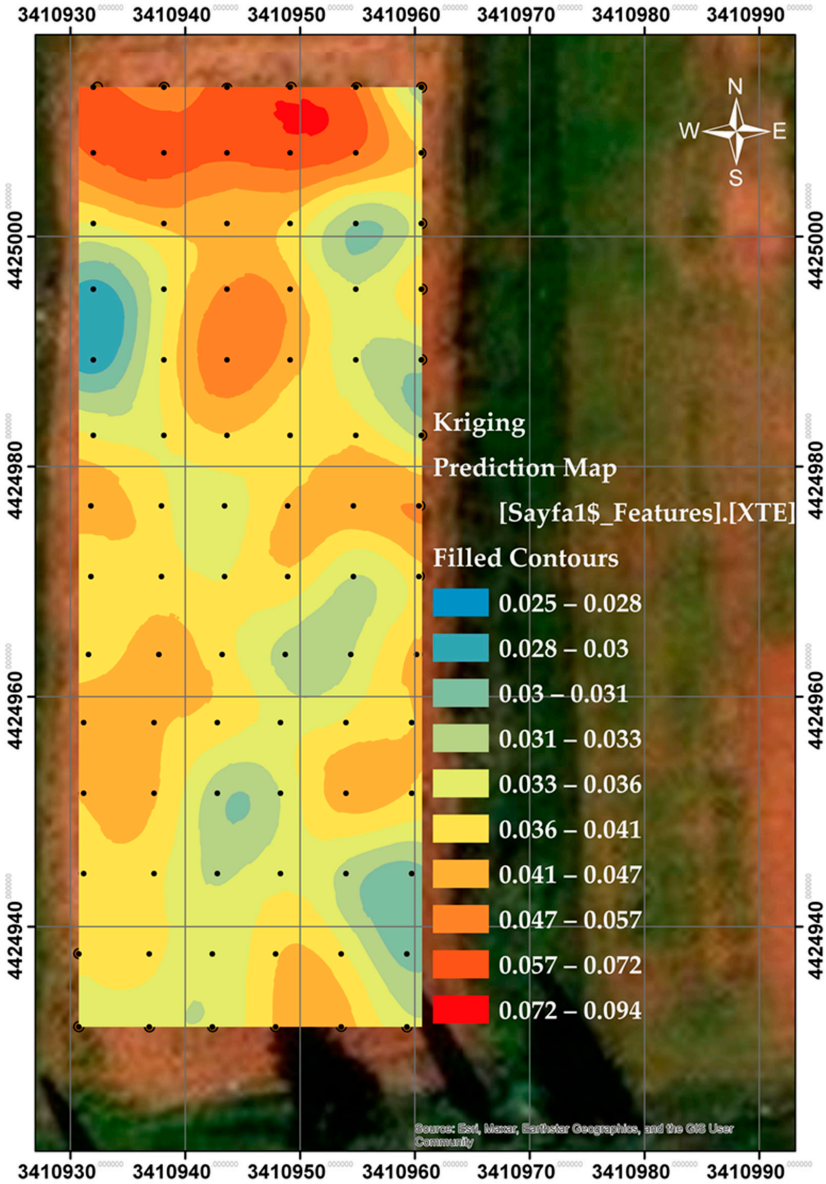


Figure 16. The spatial distribution of the XTE. This spatial distribution map represents the correlation between XTE values and the all locations of the study field.

Efficiency is a crucial indicator of the performance of agricultural robotic systems. The developed GIS-based autonomous soil-drilling robot has been evaluated to determine whether it meets the efficiency requirements. The continuous operating time of the robot is a key metric, and it is determined by the battery capacity and energy efficiency. Based on the current drawn and operating time of each component, the robot can operate continuously for approximately 3.53 h with fully charged batteries. Additionally, the average time spent per hole, including the drilling and repositioning, is 47 s. Energy intensity, defined as the amount of energy consumed per task, has also been considered. The energy efficiency of the robot has been optimized by taking into account the power consumption of the components and the overall system design. The total power consumption of the robot is calculated by considering the energy requirements of four 250 W motors and one 500 W motor, as well as other components. The total energy consumption has been determined to be 958.695 A·s. The power supply system, consisting of two 12V-72 Ah batteries, enables the robot to operate continuously for long periods, with an estimated runtime of approximately 3.53 h with fully charged batteries.

4. Discussion

The need to modify orchard mechanization technologies to meet contemporary demands has resulted in the development of new, efficient machinery. Intensive orchards ensure favorable circumstances for large fruit production and autonomous mechanized processes. Table 2 shows that the spacing between rows varies from 2.5 to 6 m, while the spacing between trees within a row varies from 0.5 to 5.5 m depending on the planting density and culture type. In this study, the horizontal and vertical spacing between the trees for the seedling pits was determined to be six meters. Depending on the type of tree that needs to be established for the orchard, the user can adjust this predetermined distance on ArcMap software. The following stages must be completed in order to set an orchard: selecting planting material, determining spacing, field marking, digging holes, and planting trees. In this process, mechanization is needed in two stages: digging holes and planting trees. The present study focuses on a GIS-based autonomous soil-drilling robot.

Table 2. Density of planting depends on the type of culture.

Tree Name	Spacing between Rows (m)	Spacing in Rows (m)
Apple	2.5–6	0.8–5
Pear	3.5–5	1.5–4.5
Plum	5–6	3.5–4.5
Apricot	5–6	3.5–5.5
Peach	4.5–5.5	3–4
Cherry	5–7	4–5.5
Sour cherry	4–6	2–4.5
Currant	2.8–3	1–1.2
Raspberry	2.5	0.5
Blackberry	2.5	1.5–1.8
Nut	4–5	3–3.5

The majority of research on automated methods for producing tree fruits focuses on operations related to pruning and harvesting. In the literature, no GIS-based autonomous robot was found to dig holes in an orchard setup. The issue of mechanized operations must be carefully considered while building a new orchard and it must be equipped with autonomous systems and related supporting infrastructure [28]. Thus, this study is crucial for figuring out where the trees should be planted when establishing a new orchard. Because the actual location of the trees is predetermined by this technology, autonomous machines can operated for the following planting and maintenance procedures.

Mechanization is vital to agriculture as it ensures timely completion of tasks and lower costs per unit area. Today, due to the rapid development of fruit tree cultivation, horticultural practices now largely require the use of various mechanical tools. One of the most significant tools for horticulture is the soil-drilling machine. The process of preparing the planting hole takes about 30% of the total time required for mechanical seedling transplanting in horticulture [29]. This rate covers a very large amount of time in the total process. In addition to being time-consuming and physically demanding, the traditional method of digging soil can quickly cause operator fatigue. The two main categories of soil-drilling machines are hand augers and power augers. Power augers run on an engine or a drill, whereas hand augers need human labor and are best for smaller projects. There are several types of power augers, including tractor augers, gas-powered augers, and electric augers. The primary purpose of all these soil-drilling machines used in horticulture is to reduce manpower and increase horticultural productivity [30]. One of the biggest concerns with soil augers driven by gasoline engines is their transportation; because of their weight, they are very difficult to handle and they generate a lot of dust, which can be harmful to the workers' health. When all these explanations are evaluated, it is clear that the development of an autonomous soil-drilling mobile robot will result in significant benefits including lower labor costs and higher productivity per unit of time.

T-handled manual soil-drilling machines rely on human power, and the average time to dig a hole could take up to 3 to 5 min per hole. In semi-automatic machines that are powered by a motor and guided by an operator, the drilling process takes approximately 1–2 min per hole. In contrast, the developed autonomous robot can drill a hole in just 47 s, which provides much higher efficiency. In terms of energy consumption, manual machines do not consume energy directly, while semi-automatic machines with gasoline engines consume about 1 L of fuel per hour with an engine power of 2–3 HP (1.5–2.2 kW). The autonomous robot uses four 250 W motors and one 500 W motor for a total of 1.5 kW, alongside a 2.1 HP gasoline engine for drilling. This configuration makes the robot more balanced and efficient in energy consumption compared to existing semi-automatic solutions. The autonomous robot, which demonstrates satisfying performance in precision drilling and GPS-assisted navigation, can operate continuously for approximately 3.53 h with fully charged batteries. As a result, the GIS-based autonomous soil-drilling robot offers much higher efficiency in terms of labor and time compared to existing solutions on the market.

There are manual, semi-automatic, and tractor three-point connection-type soil augers on the market. A soil auger can also be powered by hand, an electric motor, or an internal combustion engine or from a tractor or other vehicle through a power take-off. Especially when it is necessary to open large amounts of holes, it is of critical importance which type of soil auger system should be used in terms of intensive labor, operating costs, and time. The comparative performances of manual, semi-automatic, and our developed mobile robot were evaluated based on field capacity. As a result of the calculations, the field capacity values for manual, semi-automatic, and mobile robot-based autonomous soil auger machines were obtained as 11.62 holes/hour, 30.04 holes/hour, and 70.38 holes/hour, respectively. The values obtained show that the mobile robot-based autonomous soil auger machine drills holes faster than the other two machines and without requiring manpower. This study can be enriched to include different agricultural management methods and cost analysis elements.

Autonomous agricultural robots and guidance systems have been the subject of several research studies. The most critical factor is location accuracy regarding the navigation of agricultural robots, in other words, the accuracy with which the mobile robot arrives at the desired location. Stombaugh et al. [31] reported that the lateral position error was 16 cm (95% confidence) on the position accuracy of high-speed mobile robots. Nagasaka et al. [32] showed that the robot deviated from the desired path by more than 12 cm maximum for an autonomous rice-transplanting robot. The authors reported that the robot's position accuracy was below 1 m. Ünal and Topakci [26] designed a remote-controlled and GPS-guided autonomous robot for precision farming. The authors reported that the linear target point precision ranged from 10 to 12 cm and the distributed target point precision ranged from 15 to 17 cm. When the studies in the literature are examined, it is understood that the location sensitivity varies between 0.1 and 1 m. In our study, the minimum and maximum XTE values were observed to be 2.41 and 9.41 cm, respectively. This shows that this study's results are better than other results in the literature.

Every orchard management operation needs a mobile platform in order to move the actuators around the orchard. Accurate mobile platform navigation is necessary in an orchard, and it must consider simultaneous manipulations towards the tree or fruits [6]. In the literature, some studies about navigating mobile systems have been conducted in orchard environments using a priori maps [33–35]. Dong et al. [36] generated a semantic map of an orchard using RGB-D cameras. The authors reported that the information is not limited to coordinates on these maps. Nevertheless, no robotic system has been used to evaluate this technology. Han et al. [37] reported that the four categories can be used to categorize the autonomous driving path definition techniques for orchards. The first approach is georeferencing aerial images to construct an autonomous driving path [38]. However, this system has a drawback about the additional costs to construct an autonomous driving path. The second approach involves first identifying the ends of fruit tree rows in order to create an autonomous driving route [39]. But the disadvantage of this

system is that an incorrect path may occur when an incorrect location is obtained due to the performance of the LiDAR or camera. The third approach involves using cameras and/or LiDAR to detect tree trunks in order to create a map of an orchard [40]. However, bad weather or lighting can cause the LiDAR or camera to collect erroneous data, which could lead to inaccurate mapping of object placements in the resultant map. The fourth approach involves obtaining location data before the field study for the autonomous driving route. However, this system has a risk of collision during autonomous driving because this system only knows the location of the road and not the trees. On the other hand, our suggested system is similar to the fourth method but has some advantages. The first advantage is that the locations of the trees in the orchard are known to the mobile robot. Secondly, it has the potential to create various route algorithms depending on the positions of known trees.

The GIS-based autonomous soil-drilling robot is equipped with an RTK-GPS system that provides centimeter-level accuracy, essential for precise drilling operations. The digital compass ensures correct orientation, enhancing the overall accuracy of the robot's movements. Additionally, the soil auger machine, powered by a 2.1 HP gasoline engine, delivers consistent drilling performance across various soil types and conditions. The robot's design ensures that it meets the high standards of precision and quality necessary for optimal orchard installation.

The total initial investment required for the GIS-based autonomous soil-drilling robot is approximately USD 5000. While this upfront cost might seem substantial, the robot offers numerous long-term benefits that can greatly outweigh the initial expenses. By significantly increasing operational efficiency and reducing the need for manual labor, the robot not only lowers labor costs but also enhances the precision of orchard installations. This precision is crucial for ensuring optimal sapling growth and health, leading to better crop yields. Additionally, the robot's efficient use of resources and automation capabilities help to minimize operational expenses over time. As a result, these combined advantages can help to recoup the initial investment and provide ongoing economic benefits to users, making the adoption of this innovative technology a financially sound decision in the long run.

In this study, the development of a GIS-based autonomous soil-drilling robot aimed to enhance the efficiency and precision of orchard installation processes. The robot successfully integrates high-precision RTK-GPS and a digital compass for accurate navigation and utilizes Landsat imagery and ArcGIS software to map drilling spots. The field tests demonstrated the robot's significant improvements in operational efficiency, precision, and reduced labor costs. Compared to manual and semi-automatic systems, our robot offers a fully autonomous, high-precision solution that enhances orchard installation processes and yields better crop outcomes. These results confirm the achievement of the stated research goals, the high-quality implementation of the technological process, and the advantages of our solution over existing ones.

5. Conclusions

The agriculture robot market is rapidly expanding and is projected to reach significant growth milestones in the coming years. As of 2024, the market value is estimated to be USD 13.5 billion. This market is expected to grow at a compound annual growth rate (CAGR) of 24.3%, reaching approximately USD 40.1 billion by 2028. In this dynamic market, a lot of robotic research is being conducted to move the fruit-growing industry forward. Robotic systems for digging seedling holes in orchards show great promise in enhancing management accuracy and efficiency, reducing labor, and yielding higher yields. Various designs and implementations demonstrate high precision and autonomy in navigation and operation, making them valuable tools for modern agriculture. These systems typically involve autonomous navigation, advanced sensing technologies, and precise control mechanisms to perform tasks traditionally performed by human labor. Horticulture automation with mobile robots is a field that is constantly evolving. Mechanized and intelligent operations are becoming more and more prevalent in the process of planting orchards, especially during the establishing phase. No published studies have been under-

taken on the use of autonomous mobile robots for orchard soil drilling. In this context, a new design for optimizing orchard planting efficiency with a GIS-integrated autonomous soil-drilling robot was presented in this paper. This proposed GIS-based autonomous soil-drilling robot meets the demands of orchards for digging holes. The developed GIS-based autonomous soil-drilling robot demonstrates significant improvements in efficiency and energy consumption compared to existing solutions. The detailed calculations show that the robot can operate continuously for approximately 3.53 h on a full charge, drilling an average of 76 holes per hour and up to 608 holes in an 8 h workday. This high efficiency is achieved with an average drilling time of 47 s per hole, significantly reducing the labor and time required compared to manual and semi-automatic methods. Additionally, it has the potential to create a variety of routing methods based on known tree positions for different orchard operations. Our study demonstrates that fruit producers need to utilize this robot to automate the labor-intensive and time-consuming task of digging seedling pits; furthermore, it promises to offer new benefits to the horticulture sector, indicating a broad impact potential.

Author Contributions: İ.Ü. was responsible for the project administration, conceptualization, data curation, formal analysis, methodology, software, and writing—original draft. O.E. was responsible for funding acquisition, investigation, resources, validation, and visualization, software, writing—original draft, and writing—review and editing. All authors have read and agreed to the published version of the manuscript.

Funding: This work is financially supported by The Scientific Research Projects Coordination Unit of Akdeniz University (project number: FDK-2024-6549).

Data Availability Statement: The original contributions presented in this study are included in the article; further inquiries can be directed to the corresponding author.

Conflicts of Interest: The authors declare no conflicts of interest.

References

1. Chi, Y.; Zhou, W.; Wang, Z.; Hu, Y.; Han, X. The Influence Paths of Agricultural Mechanization on Green Agricultural Development. *Sustainability* **2021**, *13*, 12984. [CrossRef]
2. Jiang, A.; Ahamed, T. Navigation of an Autonomous Spraying Robot for Orchard Operations Using LiDAR for Tree Trunk Detection. *Sensors* **2023**, *23*, 4808. [CrossRef] [PubMed]
3. Karunathilake, E.M.B.M.; Le, A.T.; Heo, S.; Chung, Y.S.; Mansoor, S. The Path to Smart Farming: Innovations and Opportunities in Precision Agriculture. *Agriculture* **2023**, *13*, 1593. [CrossRef]
4. Bergerman, M.; Singh, S.; Hamner, B. Results with Autonomous Vehicles Operating in Specialty Crops. In Proceedings of the IEEE International Conference on Robotics and Automation, Saint Paul, MN, USA, 14–18 May 2012; IEEE: Piscataway, NJ, USA, 2012; pp. 1829–1835.
5. Bochtis, D.; Griepentrog, H.W.; Vougioukas, S.; Busato, P.; Berruto, R.; Zhou, K. Route planning for orchard operations. *Comput. Electron. Agric.* **2015**, *113*, 51–60. [CrossRef]
6. Verbiest, R.; Ruysen, K.; Vanwalleghem, T.; Demeester, E.; Kellens, K. Automation and robotics in the cultivation of pome fruit: Where do we stand today? *J. Field Rob.* **2021**, *38*, 513–531. [CrossRef]
7. Silwal, A.; Davidson, J.R.; Karkee, M.; Mo, C.; Zhang, Q.; Lewis, K. Design, integration, and field evaluation of a robotic apple harvester. *J. Field Rob.* **2017**, *34*, 1140–1159. [CrossRef]
8. Bac, W.C.; van Henten, E.J.; Hemming, J.; Edan, Y. Harvesting robots for high-value crops: State-of-the-art review and challenges ahead. *J. Field Rob.* **2014**, *31*, 888–911. [CrossRef]
9. Onishi, Y.; Yoshida, T.; Kurita, H.; Fukao, T.; Arihara, H.; Iwai, A. An automated fruit harvesting robot by using deep learning. *Robomech J.* **2019**, *6*, 13. [CrossRef]
10. Zhang, K.; Lammers, K.; Chu, P.; Li, Z.; Lu, R. System design and control of an apple harvesting robot. *Mechatronics* **2021**, *79*, 102644. [CrossRef]
11. Xiong, Z.; Feng, Q.; Li, T.; Xie, F.; Liu, C.; Liu, L.; Guo, X.; Zhao, C. Dual-Manipulator Optimal Design for Apple Robotic Harvesting. *Agronomy* **2022**, *12*, 3128. [CrossRef]
12. Chen, K.; Li, T.; Yan, T.; Xie, F.; Feng, Q.; Zhu, Q.; Zhao, C. A Soft Gripper Design for Apple Harvesting with Force Feedback and Fruit Slip Detection. *Agriculture* **2022**, *12*, 1802. [CrossRef]
13. Gonzalez Nieto, L.; Wallis, A.; Clements, J.; Miranda Sazo, M.; Kahlke, C.; Kon, T.M.; Robinson, T.L. Evaluation of Computer Vision Systems and Applications to Estimate Trunk Cross-Sectional Area, Flower Cluster Number, Thinning Efficacy and Yield of Apple. *Horticulturae* **2023**, *9*, 880. [CrossRef]

14. Liu, L.; Liu, Y.; He, X.; Liu, W. Precision Variable-Rate Spraying Robot by Using Single 3D LIDAR in Orchards. *Agronomy* **2022**, *12*, 2509. [CrossRef]
15. Botterill, T.; Paulin, S.; Green, R.; Williams, S.; Lin, J. A robot system for pruning grape vines. *J. Field Rob.* **2017**, *34*, 1100–1122. [CrossRef]
16. Jia, L.; Wang, Y.; Ma, L.; He, Z.; Li, Z.; Cui, Y. Integrated Positioning System of Kiwifruit Orchard Mobile Robot Based on UWB/LiDAR/ODOM. *Sensors* **2023**, *23*, 7570. [CrossRef] [PubMed]
17. Shalal, N.; Low, T.; McCarthy, C.; Hancock, N. Orchard mapping and mobile robot localisation using on-board camera and laser scanner data fusion—Part B: Mapping and localization. *Comput. Electron. Agric.* **2015**, *119*, 267–278. [CrossRef]
18. Cheein, F.A.; Carelli, R. Agricultural robotics: Unmanned robotic service units in agricultural tasks. *IEEE Ind. Electron. Mag.* **2013**, *7*, 48–58. [CrossRef]
19. Li, X.; Yue, J.; Wang, S.; Luo, Y.; Su, C.; Zhou, J.; Xu, D.; Lu, H. Development of Geographic Information System Architecture Feature Analysis and Evolution Trend Research. *Sustainability* **2024**, *16*, 137. [CrossRef]
20. Yadav, N.; Rakholia, S.; Yosef, R. Decision Support Systems in Forestry and Tree-Planting Practices and the Prioritization of Ecosystem Services: A Review. *Land* **2024**, *13*, 230. [CrossRef]
21. Javaid, K.; Qureshi, S.N.; Masoodi, L.; Sharma, P.; Fatima, N.; Saleem, I. Orchard designing in fruit crops. *J. Pharmacogn. Phytochem.* **2017**, *6*, 1081–1091.
22. Haque, M.A.; Sakimin, S.Z. Planting Arrangement and Effects of Planting Density on Tropical Fruit Crops—A Review. *Horticulturae* **2022**, *8*, 485. [CrossRef]
23. Murcia, H.F.; Tilaguy, S.; Ouazaa, S. Development of a Low-Cost System for 3D Orchard Mapping Integrating UGV and LiDAR. *Plants* **2021**, *10*, 2804. [CrossRef] [PubMed]
24. Carballada, A.M.; Balsa-Barreiro, J. Geospatial Analysis and Mapping Strategies for Fine-Grained and Detailed COVID-19 Data with GIS. *ISPRS Int. J. Geo-Inf.* **2021**, *10*, 602. [CrossRef]
25. Pica, A.D.; Boja, F.; Teuşdea, A.; Fora, C.; Moatar, M.; Boja, N. The Usage Motor Drill in Forestry Planting. Actual Tasks on Agricultural Engineering. In Proceedings of the 48th International Symposium, Zagreb, Croatia, 2–4 March 2021; pp. 237–248.
26. Ünal, İ.; Topakci, M. Design of a Remote-controlled and GPS-guided Autonomous Robot for Precision Farming. *Int. J. Adv. Robot. Syst.* **2015**, *12*, 194. [CrossRef]
27. Sharp, I.; Yu, K. Positional accuracy measurement and error modeling for mobile tracking. *IEEE Trans. Mobile Comput.* **2012**, *11*, 1021–1032. [CrossRef]
28. Lei, X.; Yuan, Q.; Xyu, T.; Qi, Y.; Zeng, J.; Huang, K.; Sun, Y.; Herbst, A.; Lyu, X. Technologies and Equipment of Mechanized Blossom Thinning in Orchards: A Review. *Agronomy* **2023**, *13*, 2753. [CrossRef]
29. El-Gendy, H.; Abd El-Halim, S.; Morghany, H.; Aboukarima, A. Evaluating performance of a post hole digger. *J. Soil Sci. Agric. Eng.* **2009**, *34*, 5783–5793. [CrossRef]
30. Kaur, B.; Mansi; Dimri, S.; Singh, J.; Mishra, S.; Chauhan, N.; Kukreti, T.; Sharma, B.; Singh, S.P.; Arora, S.; et al. Insights into the harvesting tools and equipment's for horticultural crops: From then to now. *J. Agric. Food Res.* **2023**, *14*, 100814. [CrossRef]
31. Stombaugh, T.S.; Benson, E.R.; Hummel, J.W. Guidance Control of Agricultural Vehicles at High Field Speeds. *Trans. ASAE.* **1999**, *42*, 537–544. [CrossRef]
32. Nagasaka, Y.; Umeda, N.; Kanetai, Y.; Taniwaki, K.; Sasaki, Y. Autonomous guidance for rice transplanting using global positioning and gyroscopes. *Comput. Electron. Agric.* **2004**, *43*, 223–234. [CrossRef]
33. Paton, M.; Pomerleau, F.; MacTavish, K.; Ostafew, C.J.; Barfoot, T.D. Expanding the Limits of Vision-based Localization for Long-term Route-following Autonomy. *J. Field Robot.* **2017**, *34*, 98–122. [CrossRef]
34. Gu, Y.; Ohi, N.; Lassak, K.; Strader, J.; Kogan, L.; Hypes, A.; Harper, S.; Hu, B.; Gramlich, M.; Kavi, R.; et al. Cataglyphis: An autonomous sample return rover. *J. Field Robot.* **2018**, *35*, 248–274. [CrossRef]
35. Kragh, M.; Underwood, J. Multimodal obstacle detection in unstructured environments with conditional random fields. *J. Field Robot.* **2020**, *37*, 53–72. [CrossRef]
36. Dong, W.; Roy, P.; Isler, V. Semantic mapping for orchard environments by merging two-sides reconstructions of tree rows. *J. Field Robot.* **2020**, *37*, 97–121. [CrossRef]
37. Han, J.-h.; Park, C.-h.; Jang, Y.Y.; Gu, J.D.; Kim, C.Y. Performance Evaluation of an Autonomously Driven Agricultural Vehicle in an Orchard Environment. *Sensors* **2022**, *22*, 114. [CrossRef] [PubMed]
38. Gonzalez-de-Santos, P.; Ribeiro, A.; Fernandez-Quintanilla, C.; Lopez-Granados, F.; Brandstoetter, M.; Tomic, S.; Pedrazzi, S.; Peruzzi, A.; Pajares, G.; Kaplanis, G.; et al. Fleets of robots for environmentally-safe pest control in agriculture. *Precis. Agric.* **2017**, *18*, 574–614. [CrossRef]
39. Bayar, G. Long distance autonomous trajectory tracking for an orchard vehicle. *Ind. Robot.* **2013**, *40*, 27–40. [CrossRef]
40. Qin, J.; Wang, W.; Mao, W.; Yuan, M.; Liu, H.; Ren, Z.; Shi, S.; Yang, F. Research on a Map-Based Cooperative Navigation System for Spraying–Dosing Robot Group. *Agronomy* **2022**, *12*, 3114. [CrossRef]

Disclaimer/Publisher's Note: The statements, opinions and data contained in all publications are solely those of the individual author(s) and contributor(s) and not of MDPI and/or the editor(s). MDPI and/or the editor(s) disclaim responsibility for any injury to people or property resulting from any ideas, methods, instructions or products referred to in the content.